Available online at www.sciencedirect.com
ScienceDirect
Chinese Journal of Natural Medicines 2021, **19**(3): 170-180
doi: 10.1016/S1875-5364(21)60018-3
Chinese Journal of Natural Medicines

•Research article•

Ligustroflavone ameliorates CCl_4-induced liver fibrosis through down-regulating the TGF-β/Smad signaling pathway

KANG Rong[1, 2], TIAN Wen[1], CAO Wei[2, 3], SUN Yang[1], ZHANG Hui-Nan[1], FENG Ying-Da[1], LI Chen[1], LI Ze-Zhi[3], LI Xiao-Qiang[1*]

[1] *Key Laboratory of Gastrointestinal Pharmacology of Chinese Materia Medica of the State Administration of Traditional Chinese Medicine, Fourth Military Medical University, Xi'an 710032, China;*
[2] *Department of Natural Medicine and Institute of Materia Medica, Fourth Military Medical University, Xi'an 710032, China;*
[3] *Shaanxi Key Laboratory of Natural Products & Chemical Biology, Northwest A&F University, Yangling 712000, China*

Available online 20 Feb., 2021

[ABSTRACT] Liver fibrosis is a pathological process characterized by excess deposition of extracellular matrix (ECM) that are mainly derived from activated hepatic stellate cells. Previous studies suggested that ligustroflavone (LF) was an ingredient of *Ligustrum lucidum* Ait. with activities of anti-inflammation and anti-oxidation. In this study, we investigated whether LF had any effect on liver fibrosis. In our study, we established a mouse model of carbon tetrachloride (CCl_4)-induced liver fibrosis and used TGF-β_1-stimulated human hepatic stellate cell line (LX-2) to explore the effect of LF and associated underlying mechanism. LF was used *in vivo* with low dose (L-LF, 5 mg·kg^{-1}, i.p., 3 times each week) and high dose (H-LF, 20 mg·kg^{-1}, i.p., 3 times each week) and *in vitro* (25 μmol·L^{-1}). Histopathological and biochemical assays investigations showed that LF delayed the formation of liver fibrosis; decreased AST, ALT activities and increased Alb activity in serum; decreased MDA level, Hyp content and increased GSH-Px concentration, SOD activity in liver tissues. Moreover, immunohistochemical, immunofluorescent and Western blot results showed that LF reduced the expressions of hepatic stellate cells specific marker proteins, including collagen I and α-SMA *in vivo* and *in vitro*. In addition, LF markedly suppressed TGF-β_1-upregulated protein expressions of TβR I, TβR II, P-Smad2, P-Smad3 and Smad4 in LX-2 cells. Taken together, these findings demonstrated LF could decrease histopathological lesions, ameliorate oxidative injury, attenuate CCl_4-induced liver fibrosis, which may be associated with down-regulating the TGF-β/Smad signaling pathway.

[KEY WORDS] Ligustroflavone; Liver fibrosis; HSCs; TGF-β/Smad
[CLC Number] R965 **[Document code]** A **[Article ID]** 2095-6975(2021)03-0170-11

Introduction

Liver fibrosis is a common characteristic of chronic liver diseases in the world, and it is mostly caused by viral hepatitis, alcoholism, metabolic agents, and steatohepatitis developed from chronic liver injury [1]. Liver fibrosis is a wound-healing response presented by a massive production and deposition of extracellular matrix (ECM) [2-3]. Hepatic stellate cells (HSCs), the major mesenchymal cells in liver and the source of fibrogenic cells, play a vital role in the pathogenesis of hepatic fibrosis. Activation of HSCs is mediated by various cytokines and reactive oxygen species released from the damaged hepatocytes. HSCs undergo a process of transdifferentiation from the quiescent cells to myofibroblasts, which produces the main components of ECM, such as collagen type I and α-smooth muscle actin (α-SMA) [4-6]. Type I collagen accumulation is a common hallmark of fibrotic diseases in various organs including the liver [7]. Fibroblasts are also generated from epithelial cells and HSCs through epithelial-mesenchymal transition (EMT) [8]. The proteomic features of EMT include the loss of epithelial cell adhesion molecules such as epithelial E-cadherin, which are replaced by the mesenchymal markers, α-SMA, matrix metalloproteinase (MMP)-2, MMP-9, collagens, and the intermediate filament protein vimentin [9-11].

HSCs can be activated by numerous growth factors and inflammatory cytokines, such as platelet-derived growth factor (PDGF)-BB and TGF-β_1. Among them, TGF-β_1 is the

[Received on] 23-Apr.-2020
[Research funding] This work was supported by the National Natural Science Foundation of China (Nos. 81770432 and 81970245) and the Science and Technology Program of Shaanxi Province, China (Nos. 2019PT-23 and 2019ZDLSF04-03-01).
[*Corresponding author] Tel/Fax: 86-29-84772221, E-mail: xxqqli@fmmu.edu.cn
These authors have no conflict of interest to declare.

most effective cytokine for the transformation and proliferation of HSCs [12]. TGF-*β*/Smad signaling pathway plays a key role in the progression of liver fibrosis by promoting transdifferentiation and migration of HSCs [13]. Thus, blocking TGF-*β*/Smad signaling pathway may serve as an effective strategy for inhibiting activation of HSCs [14]. The activated HSCs are major targets for antifibrotic therapy. If the activation of HSCs can be inhibited, or even the activation state of HSCs can be reversed to a static state, it can provide an effective clinical treatment of liver fibrosis.

Ligustri Lucidi Fructus (LLF), the fruit of *Ligustrum lucidum* Ait. is a major component among kidney-tonifying herbal prescriptions [15]. Modern pharmacological studies have found that LLF has antioxidant [16], anti-osteoporosis [17], anti-tumor effects [18] and so on. Ligustroflavone (LF) is a natural flavonoid glycoside from the LLF. This compound provides significant pharmacological properties, including anti-inflammatory [19], and anti-complementary effects [20]. In addition, LF is a calcium-sensing receptors (CaSR) antagonist and has protective effects against diabetic osteoporosis in mice [21]. LF can also reduce necroptosis in rats' brains after ischemic stroke through targeting RIPK1/RIPK3/MLKL pathway [22]. However, the effects of LF on liver fibrosis, thus far, have not been reported.

Therefore, in this study we investigated the antifibrotic effects LF on the human hepatic stellate cell line LX-2 and

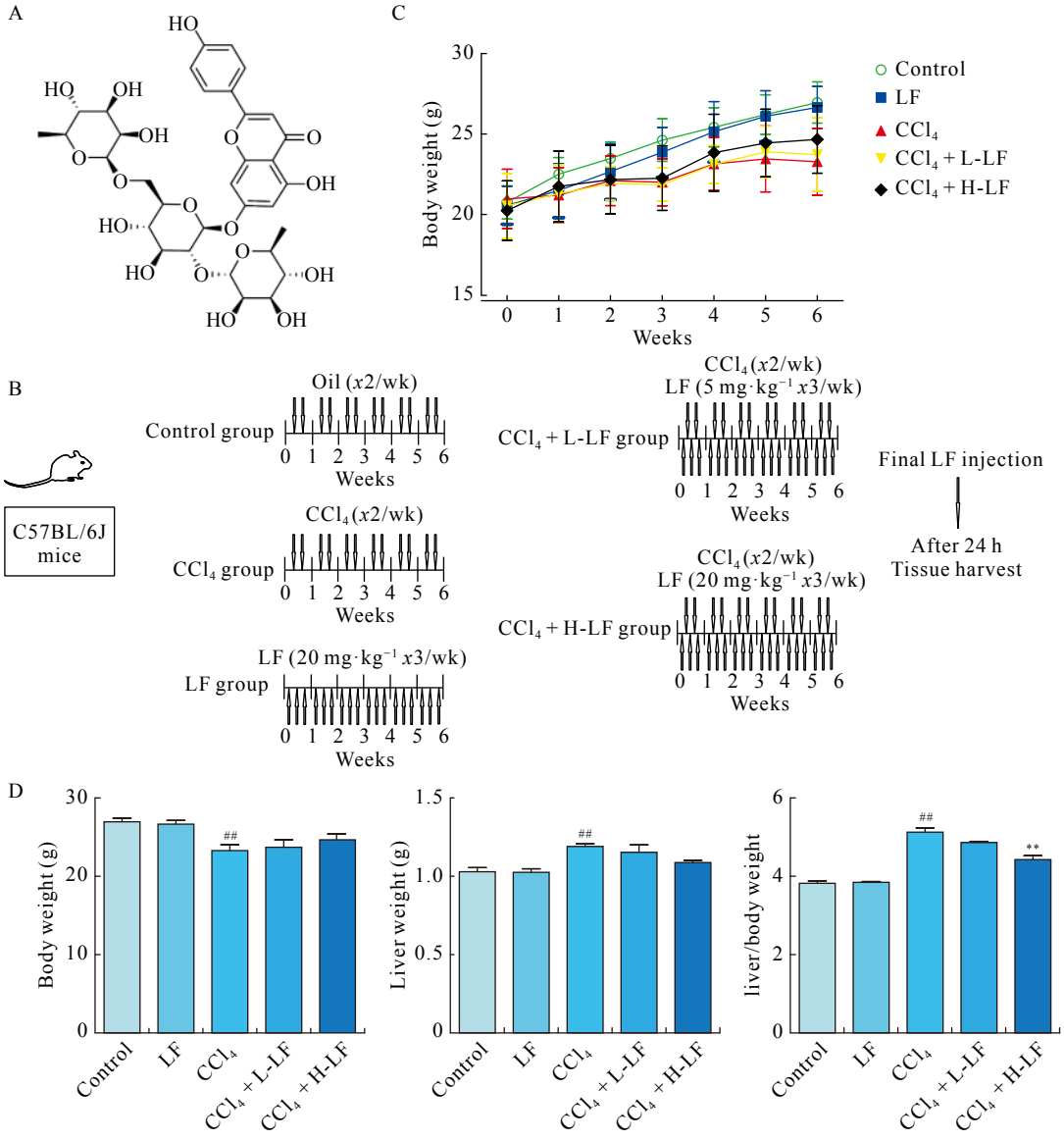

Fig. 1 LF protected against in CCl_4-induced liver injury. (A) The molecular structure of LF. (B) Schematic representation of the liver fibrosis model in C57BL/6J mice induced by intraperitoneal CCl_4 (diluted at 1∶4 in olive oil) that was administered twice a week for 6 weeks. Meanwhile, LF was intraperitoneally injected with for 6 weeks. (C) The time course of the body weight gained during the experiment. (D) body weight, liver weight, liver/body weight. Results were shown as the means ± SEM (n = 6–7). $^{*}P$ < 0.05, $^{**}P$ < 0.01 *vs* the CCl_4 group; $^{\#}P$ < 0.05, $^{\#\#}P$ < 0.01 *vs* control group

carbon tetrachloride (CCl_4)-induced hepatic fibrosis in mice and elucidated the potential mechanisms underlying its function *in vitro* and *in vivo*.

Materials and Methods

Induction of hepatic fibrosis by CCl_4

Male C57BL/6J mice (twenty-eight male, weighing between 18 g and 22 g) were supplied by the Experimental Animal Research Center of the Fourth Military Medical University (FMMU). The animals were kept under room temperature (25 ± 1 °C), atmospheric moisture (50% ± 10%), a regular 12-hour dark-light cycle, and were fed with standard laboratory food and water. To create animal models of liver fibrosis, C57 mice were intraperitoneally (i.p.) injected with CCl_4 (diluted at 1 ∶ 4 in olive oil) or olive oil alone (2 mL/kg body weight) twice a week for 6 weeks [23]. Mice were randomly divided into five groups (n = 7/group); (i) Control group; (ii) LF group; (iii) CCl_4 group and (iv) CCl_4 + L-LF group; (v) CCl_4 + H-LF group; We used two different doses of LF to assess its efficacy. Mice were administered LF with low dose (L-LF, 5 mg·kg^{-1}) and high dose (H-LF, 20 mg·kg^{-1}) [21] by intraperitoneal injection for 6 weeks, either alone or after CCl_4 administration. Mice were then sacrificed 24 h after the last injection of LF. Blood samples were collected from the orbit of the mice for further biochemical analysis. Some portions of liver tissues were fixed in 10% formalin for paraffin preparation while other portions were snap-frozen in liquid nitrogen and then stored at −80 °C until use. All animal study procedures were verified by the Institutional Animal Care and Use Committee of FMMU and were performed according to the approved guidelines.

Biochemical analysis assay

Serum activities of alanine aminotransferase (ALT), aspartate aminotransferase (AST) and albumin (Alb) were detected to assess liver function. The glutathione peroxidase (GSH-Px) concentration, superoxide dismutase (SOD) activity and malondialdehyde (MDA) level in liver tissues were measured to estimate the lipid peroxidation products and antioxidants. As a major component of collagen proteins, Hydroxyproline (Hyp) content was used to assess the degree of liver fibrosis. They were all measured with commercial kits (Nanjing Jiancheng Bioengineering Institute, Nanjing, China) using a half-automatic biochemical analyser, according to the manufacturer's instructions.

Tissue sectioning and histopathology

The fixed paraffin tissues were dehydrated in a graded ethanol series and were embedded in paraffin wax. Tissues were placed on glass slides, and paraffin was removed with xylene. Then, the tissue sections were subjected to haematoxylin and eosin, Masson's Trichrome and Sirius Red staining to evaluate the severity of fibrosis. Examinations were performed and photographs were captured with a light microscope (DM2000 LED, Leica, Solms, Germany). Image J software (National Institutes of Health, Maryland, USA) was used to calculate the ratio of the area with positive expression to the total field of Masson's Trichrome and Sirius Red staining.

Immunohistochemistry staining

Liver specimens fixed in 10% buffered formalin were embedded in paraffin blocks. Liver sections were then processed using a standard immunostaining protocol. After routine deparaffinization, blocked endogenous peroxidase was treated with 0.3% H_2O_2 for 10 min and blocked in 5% BSA for 60 min. Then, the sections were incubated with anti-α-SMA antibody (1 ∶ 100, Abcam, MA, USA) or anti-COL 1A1 antibody (1 ∶ 200, Santa Cruz Biotechnology, Texas, USA) overnight at 4 °C, and were incubated with biotin-conjugated goat anti-mouse IgG for 1 h at room temperature. The sections were incubated with the SABC (Streptavidin Biotin complex, Boster, USA) for 30 min, developed with DAB (3,3′-diaminobenzidine, Boster, USA) and counterstained with haematoxylin. The sections were observed and photographed with a microscope. Image J software (NIH) was used to calculate the ratio of the area with positive expression to the total field of α-SMA and COL 1A1 Immunohistochemistry staining.

Cell culture

The human immortalized HSC LX-2 cells was obtained from Prof. YUE Zhen-Sheng, Department of Hepatobiliary Surgery, Xijing Hospital of FMMU. The cells were cultured in High Glucose DMEM (HyClone, Utah, USA) supplemented with 10% FBS (Gibco, California, USA), 100 U·mL^{-1} penicillin and 100 μg·mL^{-1} streptomycin (Solarbio, Beijing, China) at 37 °C and 5% CO_2 in a fully humidified atmosphere.

Immunofluorescence staining

5 ng·mL^{-1} TGF-β_1 was added in a medium of LX-2 cells with LF (25 μmol·L^{-1}) for 24 h. After incubation, the cells were fixed in 4% paraformaldehyde in PBS for 10 min and were permeabilized with 0.3% Triton X-100 in PBS for 15 min at room temperature. Nonspecific binding sites were blocked by incubating the cells with 2% bovine serum albumin for 1 h. The fixed cells were incubated with a primary antibody against α-SMA (1 ∶ 100, Abcam), COL 1A1 (1 ∶ 200, Santa Cruz Biotechnology) overnight at 4 °C, followed by incubation with fluorescence (FITC)-conjugated goat anti-rabbit IgG (1 ∶ 50, Cowin Biosciences, Beijing, China) for 70 min at room temperature. The cellular nuclei were stained with DAPI for 10 min. All samples were imaged with a light microscope (DM2000 LED, Leica). Image J software (NIH) was used to calculate the ratio of the area with positive expression to the total field of α-SMA and COL 1A1.

Western blotting

Protein from each sample was subjected to 8%–10% SDS-PAGE by electrophoresis under reducing conditions and was transferred to NC membrane (Pall Gelman Laboratory, USA). The blotted membrane was then blocked with 5% skim milk or 5% BSA for 1 h at room temperature and was incubated respectively with α-SMA antibodies (1 ∶ 200, Ab-

cam), COL 1A1 (1 ∶ 200, Santa Cruz Biotechnology), P-Smad2 (1 ∶ 1000, Cell Signaling Technology, Massachusetts, USA), P-Smad3 (1 ∶ 1000, CST), Smad2 (1 ∶ 500, CST), Smad3 (1 ∶ 1000, CST), TβR I (1 ∶ 1000, Wanleibio, Shenyang, China), TβR II (1 ∶ 1000, Wanleibio), Smad4 (1 ∶ 1000, Wanleibio), Vimentin (1 ∶ 2000, Proteintech, Wuhan, China), *E*-cadherin (1 ∶ 5000, Proteintech) and β-actin (1 ∶ 5000, Beyotime Biotechnology, Shanghai, China) overnight at 4 °C. The membranes were washed three times in TBST and were incubated with goat anti-mouse/rabbit conjugated Horseradish Peroxidase (HRP) secondary antibody (1 ∶ 5000, Proteintech) for 1 h at room temperature. Membranes were visualized using ECL method (4A Biotech, Beijing, China). The intensity value of the protein bands was quantified with Image J software (NIH).

Statistical analysis

Data are expressed as the Mean ± standard error of mean (SEM). Difference between multiple groups was analyzed by one-way ANOVA with Tukey's post-hoc tests. Difference was considered to be statistically significant when *P*-value < 0.05.

Results

LF protected against in CCl_4-induced liver injury

To explore the role of LF in the progression of liver fibrosis, we established liver fibrosis model by administering CCl_4 intraperitoneally for 6 weeks and harvested tissues after the final LF treatment with a dosage of 5, 20 mg·kg^{-1} (Fig. 1B). Fig. 1C exhibits a time course of the body weight gain for the treated mice over 6 weeks. The CCl_4 group gained less body weight than the control group, more liver weight than the control group, and the CCl_4 + L-LF group and CCl_4 + H-LF group resulted in an intermediate amount of body weight and liver gain (Fig. 1D). Compared to the CCl_4 group, the liver/body weight ratio of the CCl_4 + H-LF group has decreased by about 16% (Fig. 1D). Moreover, the results also have showed that LF had no effect on healthy mice.

LF ameliorated CCl_4-induced hepatic dysfunction and oxidative injury

ALT and AST are commonly used biomarkers for liver damage. Compared to the control group, the serum ALT and AST activities were significantly higher, while the Alb activity was significantly lower ($P < 0.01$) in the CCl_4 group. Compared to CCl_4 group, ALT and AST activities of the CCl_4 + H-LF group were respectively down-regulated about 81% and 66%, while the Alb activity of CCl_4 + H-LF group was up-regulated 1.2-fold. (Fig. 2A)

Compared to the control group, the GSH-Px concentration and SOD activity were significantly lower, and MDA level was significantly higher ($P < 0.01$) in the CCl_4 group. Additionally, compared to the CCl_4 group, the results showed a significant decrease in liver MDA level in the LF high-dose

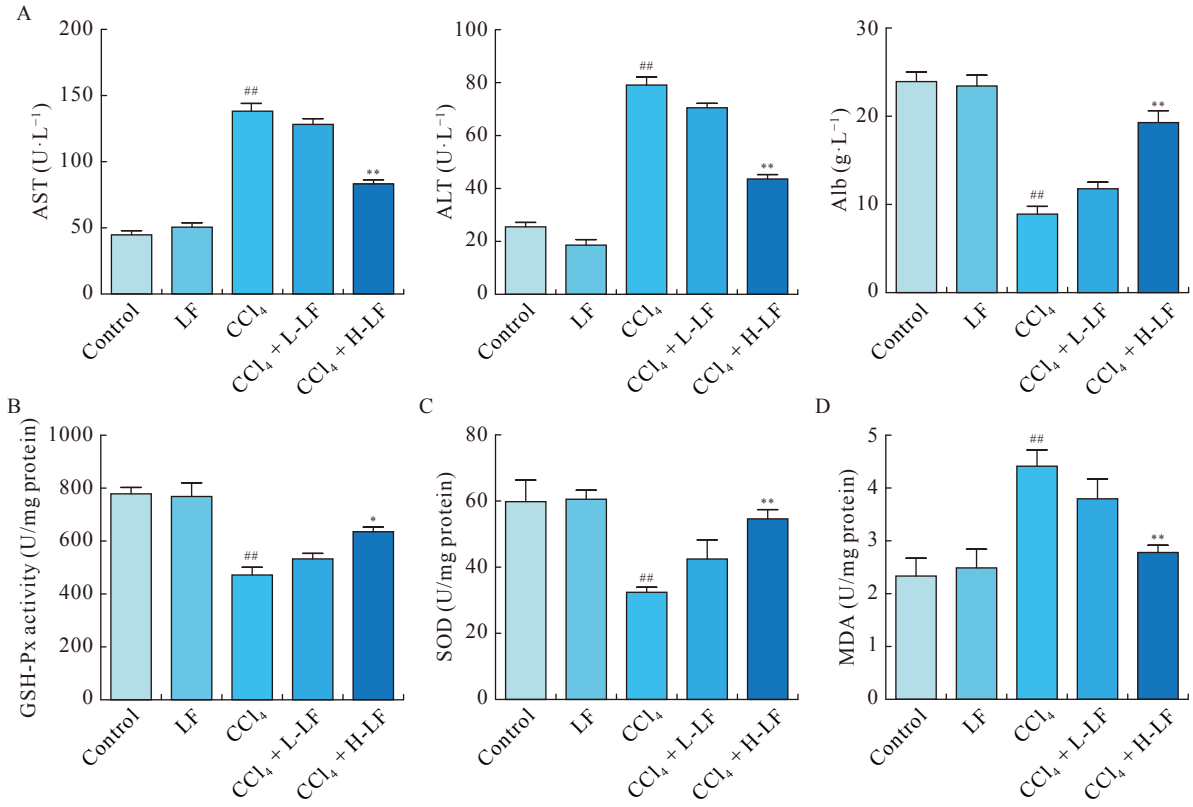

Fig. 2 LF ameliorated CCl_4-induced hepatic dysfunction and oxidative injury. (A) Serum activities of AST, ALT and Alb. (B) liver GSH-Px concentration. (C) liver SOD activity. (D) liver MDA level. Results were shown as the means ± SEM (n = 6–7). $^{*}P < 0.05$, $^{**}P < 0.01$ *vs* the CCl_4 group, $^{\#}P < 0.05$, $^{\#\#}P < 0.01$ *vs* control group

groups ($P < 0.01$). Additionally, liver GSH-Px concentration and liver SOD activity were increased significantly in the LF high-dose groups ($P < 0.05$). Moreover, the results also showed that LF had no effect on healthy mice.

LF ameliorated CCl_4-induced histological damage and liver fibrosis in liver injury

According to H&E staining (Fig. 3A), the liver tissues of the control group showed normal lobular architecture with central veins and radiating hepatic cords, with no regenerating collagen fibers. In the CCl_4 group, extensive degeneration, a dense inflammatory infiltrate, and the disappearance of the normal structure of the lobes were observed. Liver tissues in the CCl_4 + H-LF group showed significantly less necrosis of hepatic cells and less collagen deposition than the CCl_4 group.

In addition, the results of Masson's Trichrome staining (Figs. 3B and 3D) showed that collagen fibers area in the CCl_4 group was largely enhanced compared with the control group, but was markedly decreased in the CCl_4 + H-LF group ($P < 0.01$). The extent of liver fibrosis was also documented by Sirius Red staining. A marked increase in Sirius Red staining area was observed in the livers of the CCl_4 group compared with the control group (Figs. 3C and 3E). By contrast, the CCl_4-induced increase in Sirius Red staining was markedly reduced in the CCl_4 + H-LF group ($P < 0.01$). Hydroxyproline serves as a marker of collagen deposition in liver fibrosis. Compared to the control group, Hyp content in liver tissues was significantly increased in the CCl_4 group. Hyp content was decreased significantly in the CCl_4 + H-LF group compared with the CCl_4 group (Fig. 3F, $P < 0.01$). The CCl_4-induced liver injury and fibrosis were significantly attenuated in the CCl_4 + H-LF group, but the CCl_4 + L-LF group had no statistical significance. Moreover, the results also showed that LF treatment in absence of CCl_4 had no significant effects on histological changes.

LF attenuated the expressions of α-SMA and COL 1A1 in CCl_4-induced liver fibrosis

The results of immunohistochemistry showed that the positive expressions of α-SMA and COL 1A1 proteins in CCl_4 group was significantly increased, and the positive expressions of α-SMA and COL 1A1 proteins were found in central vein, hepatic sinusoid space, portal area. Compared

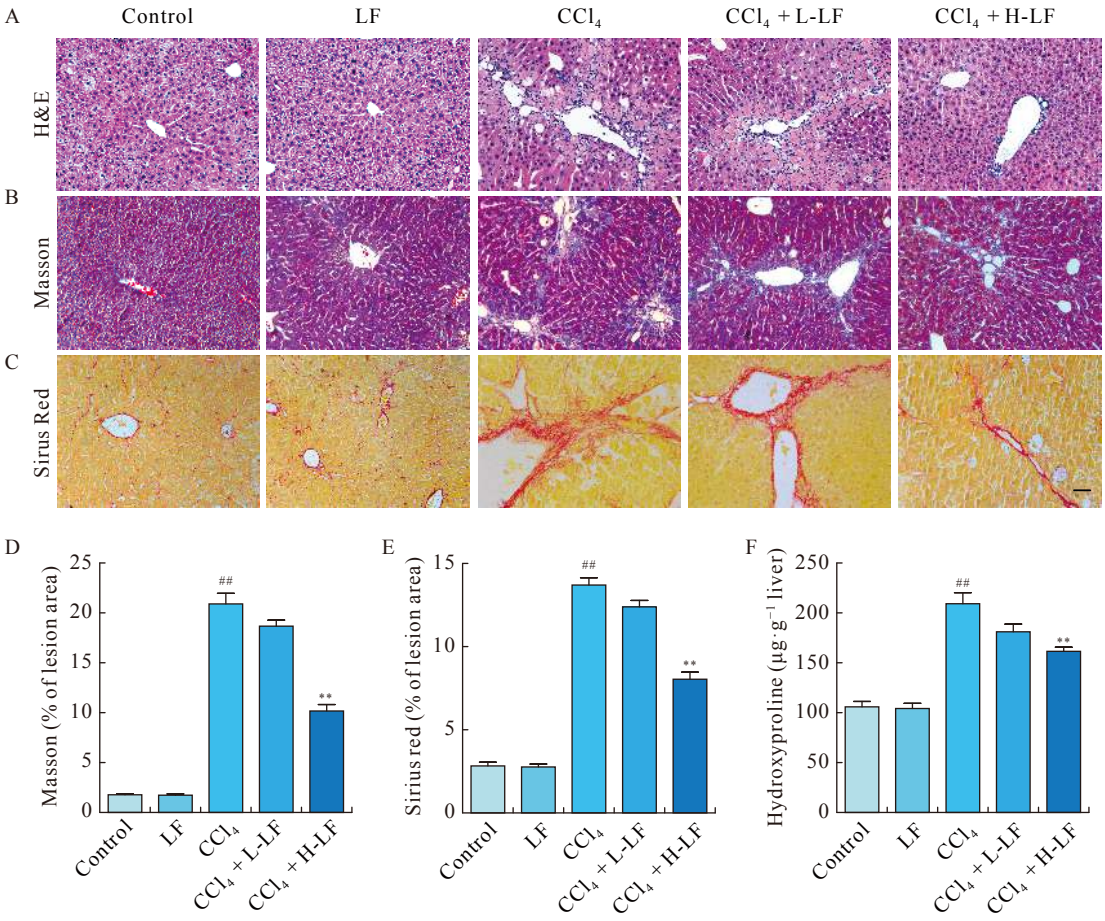

Fig. 3 LF ameliorated CCl_4-induced histological damage and liver fibrosis in liver injury. (A) H&E staining. (B) Masson staining. (C) Sirius Red staining. The scale bar is 50 μm. (D) and (E) Area density analysis of Masson's trichrome and Sirius Red staining, respectively. (F) Hyp in liver tissues was detected to analyze the effect of anti-fibrosis of LF. Results were shown as the means ± SEM (n = 6–7). $^{*}P < 0.05$, $^{**}P < 0.01$ *vs* the CCl_4 group, $^{\#}P < 0.05$, $^{\#\#}P < 0.01$ *vs* control group

with CCl_4 group, the expression of *α*-SMA and COL 1A1 proteins significantly decreased in CCl_4 + H-LF group (Figs. 4A–4D, $P < 0.01$). The histopathology, biochemical, and immunohistochemical analyses of high-dose LF treatment with CCl_4-induced liver fibrosis had significant significance. In contrast, the low-dose group did not. Therefore, the

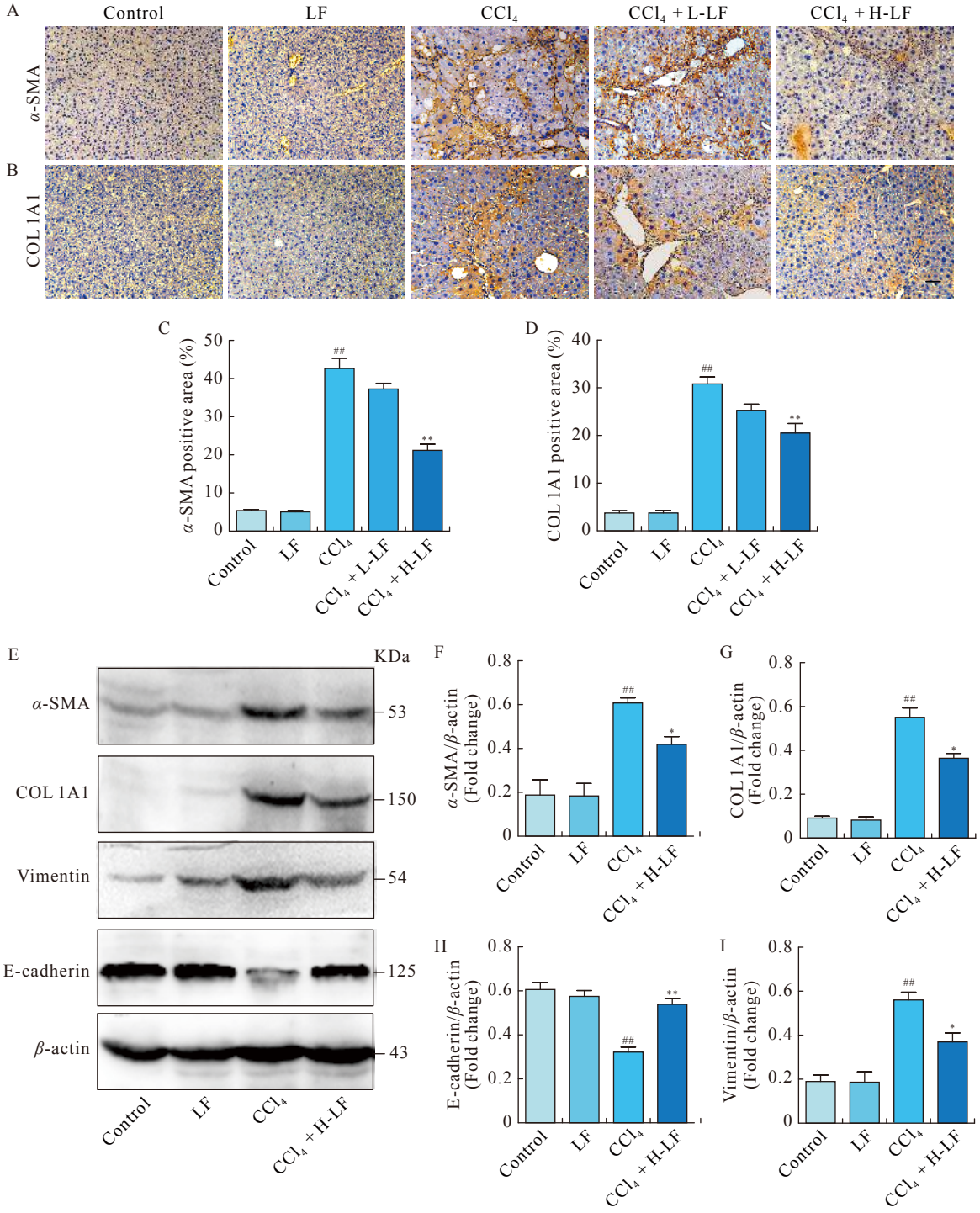

Fig. 4 LF attenuated the expressions of *α*-SMA and COL 1A1 in CCl_4-induced liver fibrosis. (A) and (B) Representative immunohistochemical staining of *α*-SMA and COL1A1. The scale bar is 50 μm. (C) and (D) Quantification of histological changes in different treatment groups with positive area using Image J analysis software (n = 6–7). (E) The protein expression of *α*-SMA, COL1A1, Vimentin and *E*-cadherin were examined by Western blots. (F), (G), (H) and (I) Quantitative analysis of COL1A1, *α*-SMA, Vimentin, E-cadherin and *β*-actin expression (n = 3). All data were presented as means ± SEM. $^{*}P < 0.05$, $^{**}P < 0.01$ *vs* the CCl_4 group, $^{\#}P < 0.05$, $^{\#\#}P < 0.01$ *vs* control group

following experiments were conducted in the 20 mg·kg^{-1} dose group (CCl_4 + H-LF).The results of WB further confirmed that the expressions of α-SMA and COL 1A1 proteins in CCl_4 + H-LF group was significantly lower than that of CCl_4 group ($P < 0.05$). Meanwhile, LF had no effect on the expression of COL 1A1 and α-SMA in the liver of healthy mice (Figs. 4E–4G). In addition, EMT has been regarded as a crucial mechanism in the progress of liver fibrosis. As shown in Fig. 4E, the results of western blot analysis showed that the protein levels of vimentin were significantly higher in the CCl_4 group compared with the control group, and the E-cadherin (Figs. 4E and 4H) level was significantly lower than that of the control group. Additionally, vimentin (Figs. 4E and 4I) levels in the CCl_4 + H-LF groups were significantly lower than in the CCl_4 group, E-cadherin levels in the CCl_4 + H-LF groups were significantly higher than in the CCl_4 group, as expected.

LF reduced the expressions of α-SMA and COL 1A1 in TGF-β_1-stimulated LX-2 cells

Immunofluorescence analysis's results showed that the α-SMA and COL 1A1 expressions were significantly higher in the TGF-β_1-stimulated group compared with the control group. Additionally, compared to the TGF-β_1-stimulated group, the α-SMA (Figs. 5A and 5C) and COL 1A1 (Figs. 5B and 5D) expressions were significantly lower ($P < 0.01$) in the TGF-β_1 + LF group. In accordance with the Immunofluorescence analysis's results, the upregulation of α-SMA and COL 1A1 by LF were further confirmed with protein levels using the Western blots. LF, when co-treated with TGF-β_1, presented the inhibitory effects on the TGF-β_1-stimulated expression of α-SMA (Figs. 5E and 5F) and COL 1A1 (Figs. 5E and 5G) proteins ($P < 0.01$) in LX-2 cells compared with the TGF-β_1-stimulated group. Treatment with LF alone did not change the state of hepatic stellate cells.

LF down-regulated TGF-β/Smad signaling pathway in vitro

As shown in Figs. 6A and 6B, western blot analysis showed that the protein expressions of TβR I, TβR II, P-Smad2, P-Smad3 and Smad4 were significantly higher in the TGF-β_1-stimulated group compared with the control group, and this effect in the LF + TGF-β_1 group was significantly lower than in the TGF-β_1-stimulated group, as expected.

Discussion

As is well known, liver fibrosis is the last reversible stage in chronic hepatopathy. However, there is lack of ideal drugs such as anti-fibrotic agents for curing hepatic fibrosis at present. Therefore, it is an urgent task to discover some effective drugs for preventing or treating liver fibrosis and investigate the mechanism of action against it. Although it is reported that flavonoid glycosides derived from LLF has anti-inflammatory property, its mechanism for the treatment of liver fibrosis is not clear. In our study, we have reported that LF has therapeutic effects on CCl_4-induced liver fibrosis and have investigated its underlying mechanism of action. The result indicated that LF modulated the TGF-β/Smad signaling pathway in reducing the expressions of hepatic stellate cells specific marker proteins against liver fibrosis during the progress of the disease.

In this study, the classical subcutaneous injection of carbon tetrachloride was used to establish the model of hepatic fibrosis in mice. It has been proved that carbon tetrachloride can directly destroy the hepatic cell membrane and cause hepatic lobular cell necrosis, resulting in hepatic fibrosis in mice [24].

According to our study, the liver of mice was observed, weighed and the organ coefficient was calculated. It is suggested that LF can improve the swelling and edema of liver in mice with hepatic fibrosis (Fig. 1D). AST and ALT are common markers of liver injury. LF can down-regulate the expression of ALT, AST and up-regulate the expression of Alb (Fig. 2A) in mice with hepatic fibrosis. These results confirmed that LF improved the liver function in CCl_4-induced liver fibrosis.

Oxidative stress is recognized as one of liver injure mechanisms related to liver fibrosis, and it accelerates collagen synthesis by activating hepatic stellate cells (HSCs) and ECM deposition through the TGF-β_1 signaling pathway during hepatic fibrosis progression [25-27]. MDA, GSH, and SOD are important indicators of oxidative stress in the liver [28]. According to our experiments, biochemical results indicated that the protective effect of LF on CCl_4-induced liver fibrosis in mice may be achieved by increasing the expression of antioxidants SOD and GSH-Px as well as reducing the level of lipid peroxide MDA. Its mechanism may be that LF contains multiple hydroxyl groups, which can provide electrons to react with free radicals, thus scavenging free radicals and inhibiting lipid peroxidation.

The effect of LF on CCl_4-induced hepatic injury and fibrosis were evaluated by H&E, Masson and Sirius Red staining (Figs. 3A–3E). Hydroxyproline, a major constituent of collagen, is a key marker for ECM accumulation. LF can down-regulate the expression of Hyp (Fig. 3F). It was found that LF could significantly prevent death of hepatocytes and cholangiocytes, decrease a large number of inflammatory cells infiltrated and aggregated in the high-dose group. As a consequence, liver fibrosis is ameliorated based on that LF reduced the area of portal area fibrosis and bridging fibrosis in the high-dose group. Under the continuous stimulation of injury factors, HSCs are transformed from a static vitamin A storage type to α-SMA expressing myofibroblasts, which are the main cells that synthesize and secrete collagen fibers. It mainly secretes type I, type III and type IV collagen, and its ability to synthesize ECM is stronger, which plays an important role in the occurrence and development of hepatic fibrosis. α-SMA is regarded as an important marker of the HSCs activation which are the primary cell type in the liver responsible for excess collagen synthesis during liver fibrosis [29]. The above results suggested that LF can down-regulate the marker of HSCs' activation (α-SMA and COL 1A1), and this may be the potential mechanism underlying its liver

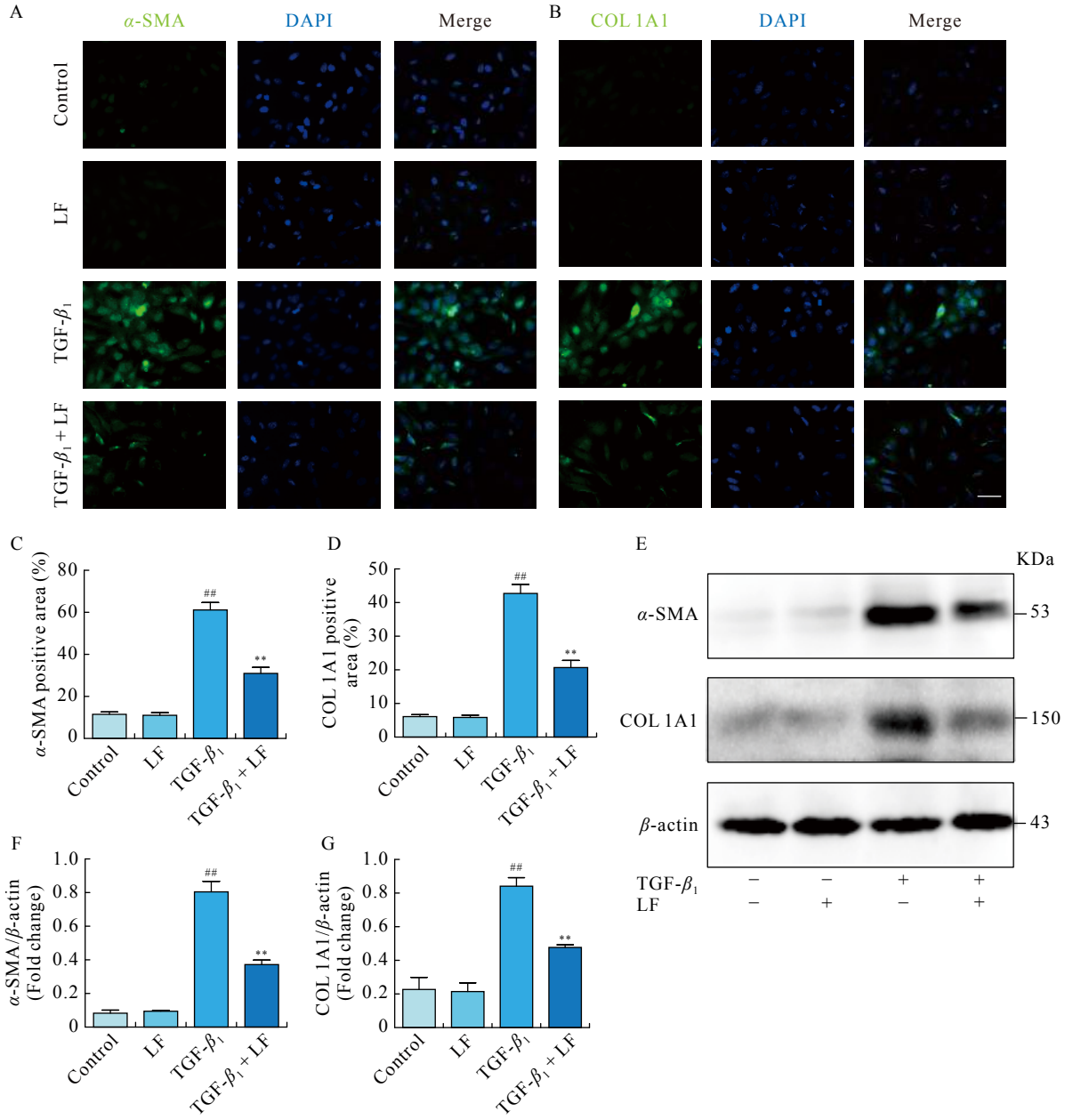

Fig. 5 LF reduced the expressions of *α*-SMA and COL 1A1 in TGF-*β*1-stimulated LX-2 cells. (A) and (B) Immunofluorescence staining of LX-2 cells with antibodies against *α*-SMA and COL 1A1. The scale bar is 50 μm. (C) and (D) The positive staining areas were measured by Image J software ($n = 5$). (E) The protein expression of *α*-SMA and COL 1A1 were examined by Western blots. (F) and (G) Quantitative analysis of COL 1A1, *α*-SMA and *β*-actin expressions ($n = 3$). All data were presented as means ± SEM. $^{*}P < 0.05$, $^{**}P < 0.01$ *vs* the TGF-β_1 treatment; $^{\#}P < 0.05$, $^{\#\#}P < 0.01$ *vs* control group

fibrosis-mitigating effect *in vitro* and *in vivo*.

Recent studies have demonstrated that ECM is not the only factor leading to liver fibrosis, and HSCs can be capable of transferring and expressing typical markers of fibroblasts by EMT and then participate in the formation of liver fibrosis [14]. Therefore, EMT is also a main part of liver fibrosis pathology [30]. In the present study, our results from Western blot analyses showed that LF attenuated the expression of EMT related protein Vimentin and up-regulated the expression of EMT related protein E-cadherin, which indicated that the inhibition of EMT could be one of the mechanisms for LF to exert its effects on liver fibrosis.

Long-term inflammation and oxidative stress caused by liver injury can lead to liver fibrosis. The morphology of HSCs can change and transform into myofibroblasts secreting many fibrosis related factors including TGF-β_1 in the process of liver injury. TGF-β_1 is one of the most important fibrosis mediators. TGF-β_1 strongly stimulates HSCs to produce collagen type I, thereby producing a large number of ECM and inhibiting ECM degradation [31]. TGF-β_1 can bind

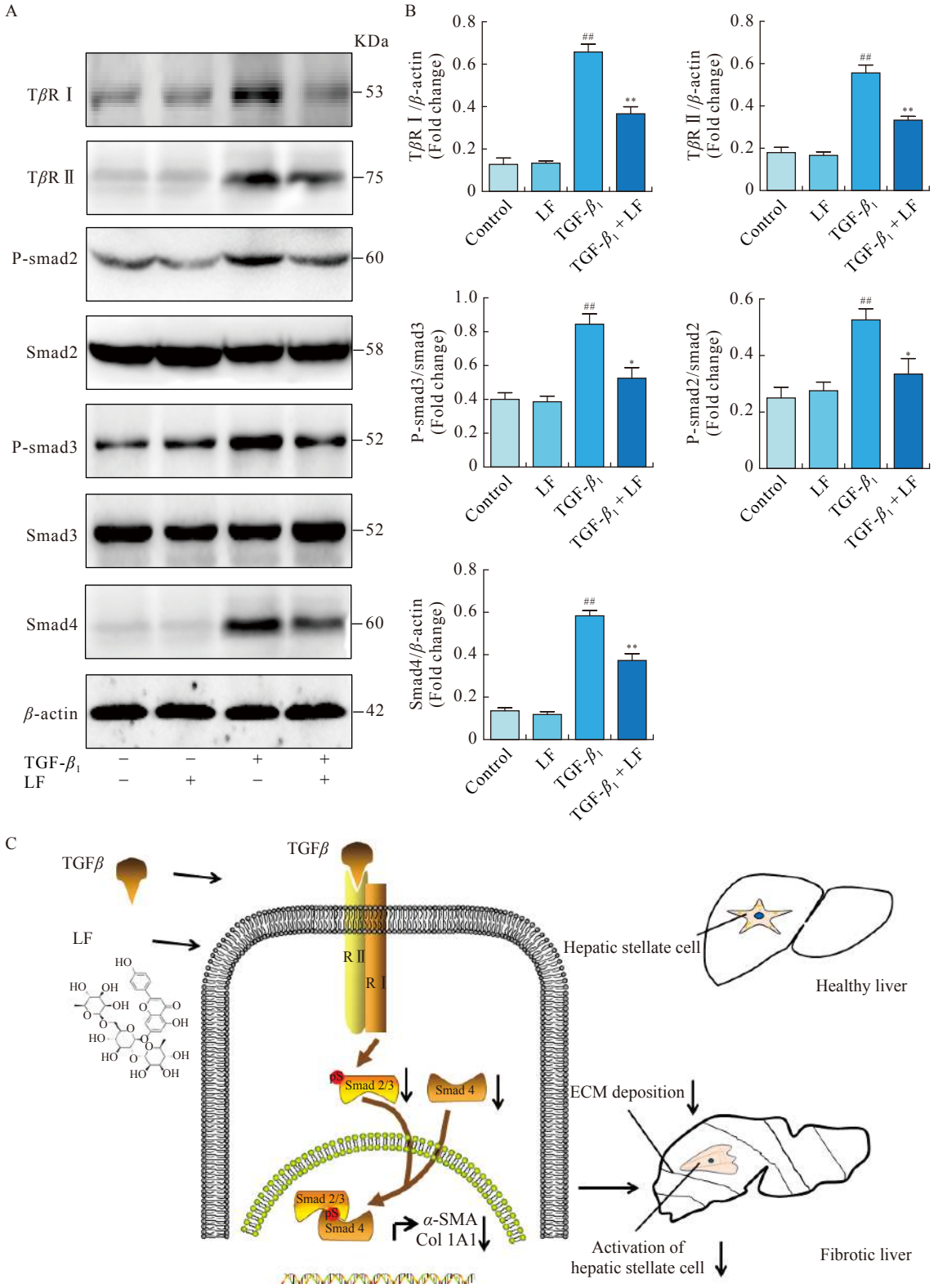

Fig. 6 LF down-regulated TGF-*β*/Smad signaling pathway *in vitro*. (A) western blot analysis for T*β*R I, T*β*R II, P-Smad2, P-Smad3, Smad4 and a loading control of (Smad2, Smad3 and *β*-actin) protein levels in LX-2 cells. (B) Quantitative analysis of T*β*R I, T*β*R II, P-smad2, P-Smad3, Smad4 and *β*-actin expressions ($n = 3$). All data were presented as means ± SEM. $^{*}P < 0.05$, $^{**}P < 0.01$ *vs* the TGF-β_1 treatment. $^{\#}P < 0.05$, $^{\#\#}P < 0.01$ *vs* the control group. (C) Schematic diagram of the antifibrotic effect of LF through down-regulating the TGF-*β*/Smad signaling pathway

to TGF-β receptor (TβR) on the HSC membrane, in which HSCs receptors include type I and type II receptors. Smads protein family, as the main effector downstream of TGF-β_1, can mediate the intracellular signal transduction of TGF-β_1 from the receptor to the nucleus. When TGF-β_1 binds to the HSCs membrane receptor and activates TβR1, activated TβR1 can phosphorylate activated Smad2 and Smad3 into P-Smad2 and P-Smad3, and form a complex of Smad2/3/4, transferring into nucleus together with Smad4 [32-34]. The transport of this complex into the nucleus enhances the expression of α-SMA and COL 1A1 and promotes fibrosis. Subsequently, we used a human immortal HSC cell line (LX-2) to more thoroughly investigate the protective mechanism. Our results showed that LF treatment was able to down-regulate TGF-β_1-induced α-SMA and COL 1A1 expressions in LX-2 cells (Fig. 5). It is due to that LF could inhibit the phosphorylation level of Smad2 and Smad3 induced by TGF-β_1 (Figs. 6A and 6B). It inhibits their entry into the nucleus, thus reducing the fibrosis activity of TGF-β_1. LF reduced the expression of hepatic stellate cells specific marker proteins, including collagen I and α-SMA, by down-regulating the TGF-β/Smad signaling pathway, so as to alleviate liver fibrosis. This further suggested that inhibition of Smad2/3 activation may be one of mechanisms of beneficial effects of LF on liver fibrosis.

According to previous reports, the pairing of Sophora flavescens and LLF ameliorated CCl_4-induced histological damage and hepatic dysfunction, but the research evidence was limited, and the effective components and mechanism were not clear [35]. In our study, it was confirmed that Ligustroflavone had anti-fibrotic effects *in vivo* and *in vitro*.

We acknowledge several limitations with this study. First, our results showed that LF had a protective effect on CCl_4-induced liver fibrosis in mice, but there are other fibrosis models of different mechanisms, such as thioacetamide (TAA)-induced liver fibrosis model and bile duct ligation (BDL)-induced liver fibrosis model, which need to be further verified the mechanisms of LF effect on anti-fibrosis. Second, some changes of oxidative stress indicators of SOD activity, GSH-Px concentration and MDA level were observed in our study, indicating that the attenuation of oxidative stress also be one of the mechanisms of hepatoprotective effect of LF. Many studies have revealed that ROS is overproduced to promote hepatocyte apoptosis and activate hepatic stellate cells, when oxidative stress occurs in the liver [36]. Subsequently, the occurrence and development of liver fibrosis were regulated by activation of Nrf2, TGF-β, NF-κB and other related cytokines, signal molecules and their downstream signal pathways [37]. However, whether LF affects the occurrence of liver fibrosis through ROS remains to be further studied. Third, the hepatoprotective effect of LF was obvious which LF alleviate CCl_4-induced liver fibrosis, but we only preliminarily studied the possible mechanism. Additional works should be required to investigate more details on TGF-β/Smad signaling pathway involved in the anti-fibrogenesis of LF. It points the way to find the target protein directly acted by LF thought virtual screening and molecular docking techniques. Furthermore, if the anti-fibrosis mechanism of LF was further confirmed in the primary hepatic stellate cells and related inhibitors, which will be a comprehensive supplement to the existing studies.

Conclusion

In conclusion, LF was involved in inhibiting the occurrence of liver fibrosis, and the mechanism may be associated with the following factors: (1) The inhibition of EMT could be one of the mechanisms for LF to exert its effects on liver fibrosis. (2) The hepatoprotective effect of LF might be related to alleviation of CCl_4-induced oxidative stress. (3) LF down-regulated TGF-β/Smad signaling pathway in LX-2 based on the protein expression of Smad2/3 phosphorylation decreasing, which resulted in down-regulating the transcriptions of α-SMA and COL 1A1.

References

[1] Friedman SL. Evolving challenges in hepatic fibrosis [J]. *Nat Rev Gastroenterol Hepatol*, 2010, **7**(8): 425-436.

[2] Friedman SL. Liver fibrosis – from bench to bedside [J]. *J Hepatol*, 2003, **38**(Suppl 1): S38-53.

[3] Xiang DM, Sun W, Ning BF, *et al*. The HLF/IL-6/STAT3 feed-forward circuit drives hepatic stellate cell activation to promote liver fibrosis [J]. *Gut*, 2018, **67**(9): 1704-1715.

[4] Maher JJ, McGuire RF. Extracellular matrix gene expression increases preferentially in rat lipocytes and sinusoidal endothelial cells during hepatic fibrosis *in vivo* [J]. *J Clin Invest*, 1990, **86**(5): 1641-1648.

[5] Hernandez-Gea V, Friedman SL. Pathogenesis of liver fibrosis [J]. *Annu Rev Pathol*, 2011, **6**: 425-456.

[6] Bataller R, Brenner DA. Hepatic stellate cells as a target for the treatment of liver fibrosis [J]. *Semin Liver Dis*, 2001, **21**(3): 437-451.

[7] Inagaki Y, Okazaki I. Emerging insights into Transforming growth factor β Smad signal in hepatic fibrogenesis [J]. *Gut*, 2007, **56**(2): 284-292.

[8] Stone RC, Pastar I, Ojeh N, *et al*. Epithelial-mesenchymal transition in tissue repair and fibrosis [J]. *Cell Tissue Res*, 2016, **365**(3): 495-506.

[9] Lee JG, Kay EP. NF-κB is the transcription factor for FGF-2 that causes endothelial mesenchymal transformation in cornea [J]. *Invest Ophthalmol Vis Sci*, 2012, **53**(3): 1530-1538.

[10] Zhang Y, Wei JS, Wang H, *et al*. Epithelial mesenchymal transition correlates with CD24+CD44+ and CD133+ cells in pancreatic cancer [J]. *Oncol Rep*, 2012, **27**(5): 1599-1605.

[11] Bi WR, Xu GT, Lv LX, *et al*. The ratio of transforming growth factor-β1/bone morphogenetic protein-7 in the progression of the epithelial-mesenchymal transition contributes to rat liver fibrosis [J]. *Genet Mol Res*, 2014, **13**(1): 1005-1014.

[12] Derynck R, Zhang YE. Smad-dependent and Smad-independent pathways in TGF-β family signalling [J]. *Nature*, 2003, **425**(6958): 577-584.

[13] Yang CQ, Zeisberg M, Mosterman B, *et al*. Liver fibrosis: insights into migration of hepatic stellate cells in response to extracellular matrix and growth factors [J]. *Gastroenterology*, 2003, **124**(1): 147-159.

[14] Cho IJ, Kim YW, Han CY, *et al*. E-cadherin antagonizes transforming growth factor β1 gene induction in hepatic stellate

cells by inhibiting RhoA-dependent Smad3 phosphorylation [J]. *Hepatology*, 2010, **52**(6): 2053-2064.
[15] Gao LL, Li C, Wang ZM, *et al*. Ligustri Lucidi Fructus as a traditional Chinese medicine: a review of its phytochemistry and pharmacology [J]. *Nat Prod Res*, 2015, **29**(6): 493-510.
[16] Lin HM, Yen FL, Ng LT, *et al*. Protective effects of *Ligustrum lucidum* fruit extract on acute butylated hydroxytoluene-induced oxidative stress in rats [J]. *J Ethnopharmacol*, 2007, **111**(1): 129-136.
[17] Chen BB, Wang LL, Li L, *et al*. Fructus Ligustri Lucidi in osteoporosis: A review of its pharmacology, phytochemistry, pharmacokinetics and safety [J]. *Molecules*, 2017, **22**(9): 1469.
[18] Jeong JC, Kim JW, Kwon CH, *et al*. Fructus ligustri lucidi extracts induce human glioma cell death through regulation of Akt/mTOR pathway *in vitro* and reduce glioma tumor growth in U87MG xenograft mouse model [J]. *Phytother Res*, 2011, **25**(3): 429-434.
[19] Pieroni A, Pachaly P. Isolation and structure elucidation of ligustroflavone, a new apigenin triglycoside from the leaves of *Ligustrum vulgare* L. [J]. *Pharmazie*, 2000, **55**(1): 78-80.
[20] Pieroni A, Pachaly P, Huang Y, *et al*. Studies on anti-complementary activity of extracts and isolated flavones from *Ligustrum vulgare* and *Phillyrea latifolia* leaves (Oleaceae) [J]. *J Ethnopharmacol*, 2000, **70**(3): 213-217.
[21] Feng R, Ding F, Mi XH, *et al*. Protective effects of ligustroflavone, an active compound from *Ligustrum lucidum*, on diabetes-induced osteoporosis in mice: A potential candidate as calcium-sensing receptor antagonist [J]. *Am J Chin Med*, 2019, **47**(2): 457-476.
[22] Zhang YY, Liu WN, Li YQ, *et al*. Ligustroflavone reduces necroptosis in rat brain after ischemic stroke through targeting RIPK1/RIPK3/MLKL pathway [J]. *Naunyn Schmiedebergs Arch Pharmacol*, 2019, **392**(9): 1085-1095.
[23] Chang J, Lan T, Li C, *et al*. Activation of Slit2-Robo1 signaling promotes liver fibrosis [J]. *J Hepatol*, 2015, **63**(6): 1413-1420.
[24] Scholten D, Trebicka J, Liedtke C, *et al*. The carbon tetrachloride model in mice [J]. *Lab Anim*, 2015, **49**(1 Suppl): 4-11.
[25] Karimi J, Mohammadalipour A, Sheikh N, *et al*. Protective effects of combined Losartan and Nilotinib on carbon tetrachloride CCl_4-induced liver fibrosis in rats [J]. *Drug Chem Toxicol*, 2018, **43**(5): 468-478.
[26] Singh MP, Kang SC. Endoplasmic reticulum stress-mediated autophagy activation attenuates fumonisin B1 induced hepatotoxicity *in vitro* and *in vivo* [J]. *Food Chem Toxicol*, 2017, **110**: 371-382.
[27] Han B, Lv Z, Zhang X, *et al*. Deltamethrin induces liver fibrosis in quails *via* activation of the TGF-β1/Smad signaling pathway [J]. *Environ Pollut*, 2019, **259**: 113870.
[28] Colak E, Ustuner MC, Tekin N, *et al*. The hepatocurative effects of *Cynara scolymus* L. leaf extract on carbon tetrachloride-induced oxidative stress and hepatic injury in rats [J]. *Springerplus*, 2016, **5**: 216.
[29] Mederacke I, Hsu CC, Troeger JS, *et al*. Fate tracing reveals hepatic stellate cells as dominant contributors to liver fibrosis independent of its aetiology [J]. *Nat Commun*, 2013, **4**: 2823.
[30] Pinzani M. Pathophysiology of liver fibrosis [J]. *Dig Dis*, 2015, **33**(4): 492-497.
[31] Liu N, Feng J, Lu X, *et al*. Isorhamnetin inhibits liver fibrosis by reducing autophagy and inhibiting extracellular matrix formation *via* the TGF-β1/Smad3 and TGF-β1/p38 MAPK pathways [J]. *Mediators Inflamm*, 2019, **2019**: 6175091.
[32] Fabregat I, Moreno-Caceres J, Sanchez A, *et al*. TGF-β signalling and liver disease [J]. *FEBS J*, 2016, **283**(12): 2219-2232.
[33] Dooley S, ten Dijke P. TGF-β in progression of liver disease [J]. *Cell Tissue Res*, 2012, **347**(1): 245-256.
[34] Heldin CH, Moustakas A. Signaling receptors for TGF-β family members [J]. *Cold Spring Harb Perspect Biol*, 2016, **8**(8): a022053.
[35] Chu SH, Zhang HX, Ding LX. Efficiency of *Sophora flavescens*-Fructus Ligustri Lucidi Drug Pairs in the treatment of liver fibrosis based on the response surface method [J]. *Evid Based Complement Alternat Med*, 2019, **2019**: 8609490.
[36] Kong M, Chen XY, Lv FQ, *et al*. Serum response factor (SRF) promotes ROS generation and hepatic stellate cell activation by epigenetically stimulating NCF1/2 transcription [J]. *Redox Biol*, 2019, **26**: 101302.
[37] Lv YY, Bing QZ, Lv ZJ, *et al*. Imidacloprid-induced liver fibrosis in quails *via* activation of the TGF-β1/Smad pathway [J]. *Sci Total Environ*, 2020, **705**: 135915.

Cite this article as: KANG Rong, TIAN Wen, CAO Wei, SUN Yang, ZHANG Hui-Nan, FENG Ying-Da, LI Chen, LI Ze-Zhi, LI Xiao-Qiang. Ligustroflavone ameliorates CCl_4-induced liver fibrosis through down-regulating the TGF-β/Smad signaling pathway [J]. *Chin J Nat Med*, 2021, **19**(3): 170-180.

LI Xiao-Qiang, Ph.D., is a pharmacological professor and doctoral supervisor at Fourth Military Medical University, and the executive director of the Key Laboratory of Gastrointestinal Pharmacology of Chinese Materia Medica of the State Administration of Traditional Chinese Medicine. His main research interests are focusing on the molecular mechanism of ion channel in regulating of diseases, and the basic and applied researches on R&D of new drug in TCM and natural products. He has published 90+ papers in scientific journals such as *Basic Res Cardiol*, *Int J Biol Macromol* and *Eur J Pharmacol*.